Relationship between perforation depth and core flow efficiency

DOI:10.36909/jer.12775

Hao Liang *,**,*** , Yonggang Duan, *, Muwang Wu**, Yuxuan Liu*,*** and Tiejun Lin*

** State Key Laboratory of Oil and Gas Reservoir Geology and Exploitation, Southwest Petroleum University, Chengdu, China*

*** CNOOC (China) Limited Hainan Branch, Haikou, Hainan, China*

**** Corresponding author: lianghao8@cnooc.com.cn (H. Liang)*

liuyx_6@163.com (Y.X. Liu)

ABSTRACT

The perforation parameters have a large influence on the productivity of offshore wells. Perforation depth and core flow efficiency (CFE) are the key parameters for evaluating perforation response, but the relationship between these two parameters is seldom studied. In this paper, the perforation experiment and CFE evaluation are carried out. The results show that with the increase of confining pressure, perforation depth decreases, CFE increases, and perforation damage decreases. The CFE decreases with the increase of perforation depth, and the relationship between them satisfies the exponential function.

Keywords: Core flow efficiency; perforation depth; perforation evaluation; offshore reservoirs;

INTRODUCTION

During the development of oil and gas fields, there are many engineering problems to be solved, such as drilling (Kang & She *et al.*, 2016; Liu, 2020) , hydraulic fracturing (Hu & Li *et al.*, 2016; Wang & Hu *et al.*, 2019), etc. Perforation plays a very important role in oil and gas exploration and development. Perforation directly affects the accuracy of reservoir evaluation and well productivity, especially for offshore reservoirs. On the one hand, the perforation tunnels formed with a certain depth and radius in the reservoir rocks. On the other hand, it also causes damage to rock structures near the perforation tunnel. The researches on perforation depth and the evaluation of flow efficiency have always been the focus of perforation process analysis.

Muskat (1943) presented the first analytical treatment considering perforation condition. Other investigators used different modeling approaches to examine the flow in perforated completions (Dogulu, 1998; Ansah & Proett *et al*., 2002; Guerra & Yildiz, 2004; Gou & Guo *et al.*, 2018; Wu & Zhu *et al.*, 2020; Gou & Wang *et al*., 2020). Tariq (1987) developed a model for modeling steady-state flow in perforated completions. The non-Darcy effect was taken into account. The results indicate a significant reduction in productivity owing to a non-Darcy effect. Deo & Tarlq *et al*. (1989) studied the flow distribution around a perforation by three-dimensional finite-element modeling. The Linear and radial flow were investigated to determine which one represents downhole conditions. Jamiolahmady & Danesh *et al*. (2006) studied the flow of gas and condensate around a perforation tunnel through experiments and finite element modeling. They found that thickness-permeability values under certain conditions could be assigned to represent the two-phase flow performance. Atkinson & Monmont *et al*. (2009) proposed an analytical treatment of a 3D problem of steady-state flow in a porous medium. However, the hydraulic resistances of perforations flowing inside them as well as the crushed zones around them with impaired permeability are neglected. Jamiolahmady & Mahdiyar *et al*. (2010) focused on the steady-state flow behavior of a single-phase fluid in and around perforated tunnels including Non-Darcy flow. They found that the pressure drop inside the long perforated tunnels under high flow velocity conditions is negligible compared to that around the perforated region. Jamiolahmady & Mahdiyar *et al.* (2011) developed an effective wellbore radius for an equivalent open-hole system, which reflects the flow around a perforated well in gas condensate reservoirs. The effect of geometry and anisotropy on perforation skin is also investigated. Li & Sun *et al.* (2012) presents the 2D analytical solution of the steady-state flow model. They found that the penetration depth and anisotropic permeability are the significant factors in the flow performance of the perforated core. Pasztor & Kosztin (2015) developed a model to simulate the flow rate and the well performance for the perforated well. Their model considered the influence of penetration depth, phase angle, length of the perforated interval, the entry hole diameter, the average radius of perforation channels and the radius of the crushed zone, etc. Zhang & Deng et al. (2018) simulated the perforation process of a single perforating shaped charge, including the effects of the explosion, jet forming, and penetration. Movahedi & Vasheghani Farahani *et al*. (2019) studied the effect of different perforation geometries on single and two-phase perforated porous media. The effect of perforation length and diameter, degree of heterogeneity, on the pressure and velocity profiles were analyzed. Araki & Morita (2020) investigated perforation interaction by numerical modeling to find the optimal perforation design that yields the highest productivity while maintaining mechanical stability.

At present, many kinds of research have carried out the evaluation of perforation depth and core flow efficiency (CFE), but few are focusing on the evaluation of perforation depth and CFE at the same time, and the relationship between perforation depth and CFE is unclear. Therefore, this paper carried out a perforation experiment and evaluated the CFE. The relationship between perforation depth and CFE were analyzed based on the results.

PERFORATION EXPERIMENT

Experimental devices

The device used in this research is shown in Figure 1, which mainly includes wellbore pressure vessel, perforation unit, wellbore and pore pressure buffer, etc.

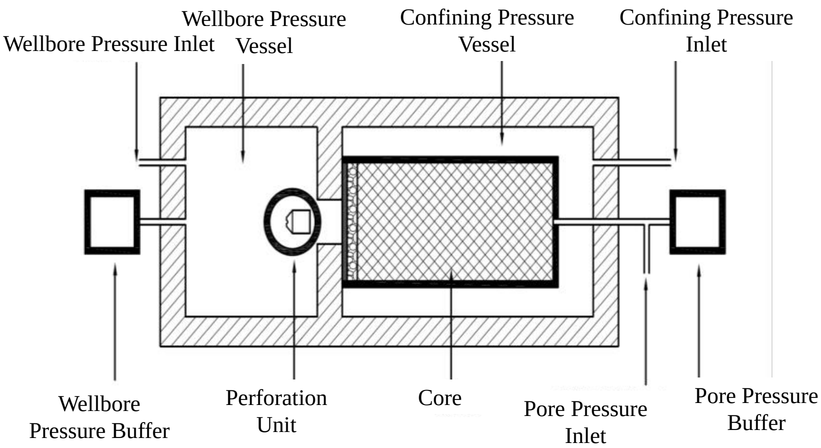

Fig. 1. Schematic diagram of the test device

The structural schematic diagram of the test device is shown in Figure 2, which mainly includes: nitrogen pressurization system, hydraulic system, heating, cooling system, controlling and monitoring system, etc., When the system works, it can perforate the sandstone target under the wellbore pressure, confining pressure and pore pressure and test the flow rate before and after perforation.

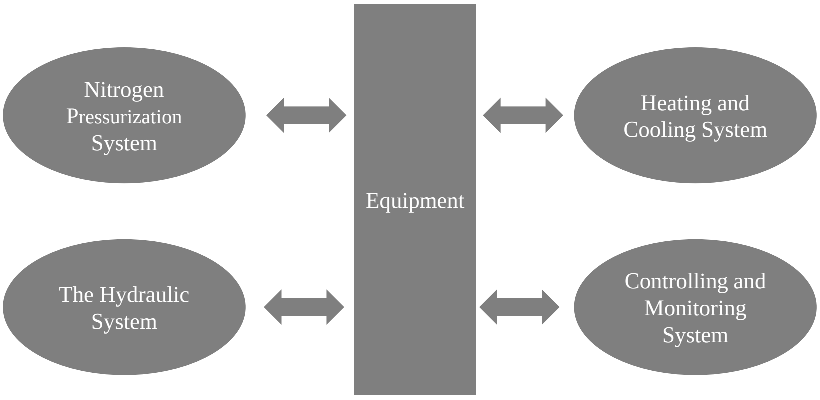

Fig. 2. Structural schematic diagram of the test system

Experimental procedures

In the study, the test of perforation and flow rate is as follows:

(1) Flow test before perforation: Measure the flow rate under steady-state flow with different pressure differences;

(2) Perforation: Install target and perforate.

(3) Flow test after perforation: According to the flow test pressure difference before perforation, recording the flow rate after the perforation.

(4) Perforation depth and radius. Cut the sandstone target laterally along the axis of the target, and measure the size of the tunnel.

The experimental scheme is shown in Table 1. Twenty-two groups of experiments were carried out, of which four types of perforation guns carried out experiments under different confining pressures and pore pressures. And the other nine types of guns were also carried out to further analyze the relationship between perforation depth and flow efficiency.

Table 1 Experimental scheme

No	Perforation gun number	Confining pressure	Poro Pressure

		(MPa)	(MPa)
1	1	25	5
2	1	30	10
3	1	35	15
4	2	20	10
5	2	25	
6	2	35	
7	3	25	5
8	3	30	10
9	3	30	10
10	3	35	15
11	4	20	10
12	4	25	
13	4	35	
14	5	30	10
15	6	30	10
16	7	30	10
17	8	30	10
18	9	30	10
19	10	30	10
20	11	30	10
21	12	30	10
22	13	30	10

Core flow efficiency evaluation

CFE is defined as the ratio between the apparent permeability measure in a core with a real damage perforation (k_p) and the permeability of a core with an ideal, clean perforation of the same perforation depth (k_i). It is calculated by:

$$CFE = \frac{k_p}{k_i} \tag{1}$$

As mentioned above, the core flow efficiency can also be simplified as the ratio of the flow rate of perforated cores to the flow rate of cores with an ideal tunnel of the same size:

$$CFE = \frac{k_p}{k_i} = \frac{q_p}{q_i} \tag{2}$$

Because the CFE excludes the influence of perforation geometry, it can truly reflect the degree of perforation damage. For example, CFE=1 means that a real tunnel is equivalent to an ideal tunnel that is completely clean and has no damage. This kind of perforation has no harm to the formation, and its CFE is the highest. When using the CFE, it is very time-consuming and inconvenient to drill an ideal tunnel and then test to find the k_i value. To calculate the CFE, it is necessary to know the ideal flow rate of the core with a tunnel. In the experiment, processes have been designed to obtain parameters such as perforation radius and length. Therefore, these data can be used to build a numerical model, and the flow rate of the ideal hole can be calculated by using the computational fluid dynamics method.

In this work, COMSOL Multiphysics was used. A three-dimensional ideal flow model is established to obtain the theoretical flow rate q_i. The size of the model is consistent with the experimental size, and the same boundary conditions are applied on both sides of the model, and then the flow field is solved. Finally, the theoretical flow rate can be calculated.

According to the simulated theoretical flow rate, the CFE of different Perforation guns can be obtained, as shown in Table 2.

Table 2 Core flow efficiency evaluation results

No	Perforation gun number	Perforation depth (mm)	Perforation radius (mm)	Experimental flow rate after perforation (cm^3/s)	Theoretical flow rate after perforation (cm^3/s)	CFE (%)
1	1	310	4.9	0.42	0.61	68.84
2	1	320	4.75	3.417	5.07	67.43
3	1	302	4.8	0.567	0.81	70.40
4	2	345	4.6	0.575	0.91	63.52
5	2	324	4.65	0.62	0.92	67.05
6	2	292	4.5	0.5283	0.73	72.50
7	3	460	4.75	1.32	2.08	46.74
8	3	430	5.15	2.90	5.72	50.66
9	3	445	5.1	0.475	0.98	48.42
10	3	440	5.1	0.523	1.06	49.15
11	4	504	4.9	0.54	1.32	40.89
12	4	436	4.8	0.4567	0.91	50.07
13	4	400	5.1	0.403	0.74	54.68

14	5	260	5.7	0.49	0.64	76.70
15	6	245	5.55	0.5767	0.81	70.97
16	7	170	5.45	2.5	1.69	98.60
17	8	325	7.9	0.45	0.71	63.11
18	9	342	5.7	0.76	0.69	62.65
19	10	387	5.85	0.665	1.19	55.94
20	11	300	7.8	0.76	0.64	66.87
21	12	240	5.25	0.123	0.15	81.10
22	13	315	7.9	0.597	0.92	64.60

It can be seen from the above table that the CFE of these perforation guns is not high, which indicates that these perforation guns have damage to the formation. Two groups of experiments adopted the same gun type with different effective confining pressures. The results of the two types of guns are shown in Figure 3.

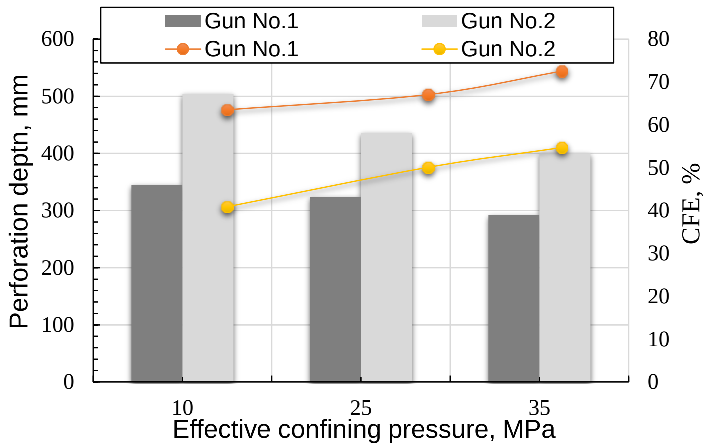

Fig. 3. Relationship between the confining pressure and perforation depth under different effective confining pressure and perforation gun

It can be seen from Figure 3 that with the increase of effective confining pressure, the perforation depth decreases, but the CFE increases. This is because the reduction of perforation depth indicates that the impact of perforation on the rocks is weakened, so the perforation damage is reduced, and then the CFE will increase. This phenomenon not only exists in these two types of guns. The perforation depth of all types of guns and the CFE is shown in Figure 4. It can be seen from the figure that with the increase of perforation depth, the CFE shows a consistent downward trend even for different types of guns.

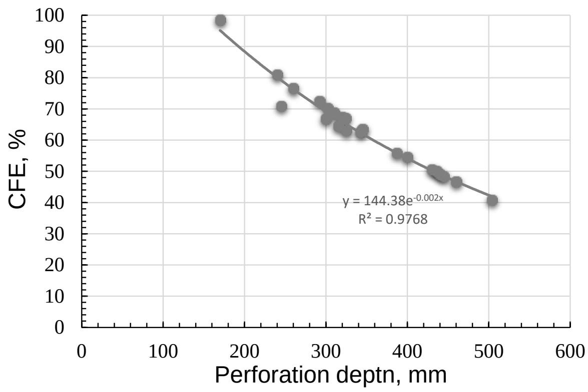

Fig. 4. Relationship between perforation depth and flow

Therefore, on the one hand, as the perforation depth increases, the production after perforating will increase. On the other hand, the perforation damage increases with the increase of perforation depth, which leads to a decrease in production. Therefore, the relationship between perforation depth and perforation damage must be considered when optimizing perforated well productivity. Otherwise, the results may overestimate the influence of perforation depth.

CONCLUSION

In this study, the relationship between perforation depth and CFE was analyzed. The results showed that:

(1) With the increase of confining pressure, perforation depth decreases, flow efficiency increases, and perforation damage decreases.

(2) With the increase of perforation depth, the flow efficiency decreases, and the relationship between perforation depth and flow efficiency satisfies the exponential function.

ACKNOWLEDGEMENTS

We thank CNOOC (China) Limited for funding and supporting this project.

NOMENCLATURE

CFE - Core flow efficiency

k_p - the permeability measure in a core with a real damage perforation, m^2

k_i- the permeability of a core with an ideal, clean perforation of the same perforation depth, m^2

q_p - the flow rate measure in a core with a real damage perforation, cm^3/s

q_i - the flow rate of a core with an ideal, clean perforation of the same perforation depth, cm^3/s

REFERENCES

Ansah, J., Proett, M.A., & Soliman, M.Y. 2002. Advances in well completion design: a new 3d finite-element wellbore inflow model for optimizing performance of perforated completions. Paper SPE 73760, presented at International Symposium and Exhibition on Formation Damage Control, Lafayette, Louisiana.

Araki, N. & Morita, N. 2020. Quantitative analysis of the effect of perforation interaction on perforation stability using the finite element method. SPE Journal, **25** (5): 2234-2250.

Atkinson, C. Monmont, F. & Zazovsky, A. 2009. Flow Performance of Perforated Completions. Transport in Porous Media, **80** (2): 305.

Deo, M., Tarlq, S.M. & Halleck, P.M. 1989. Linear and radial flow targets for characterizing downhole flow in perforations. SPE Production Engineering, **4** (3): 295-300.

Dogulu, Y. S. 1998. Modeling of Well Productivity in Perforated Completions. Paper SPE 51048, presented at SPE Eastern Regional Meeting. Pittsburgh, Pennsylvania.

Gou, B., Guo, J., & Yu, T. 2018. Modeling of quantifying proppants for stimulation reservoir volume fracturing in a shale hydrocarbon reservoir. Journal of Geophysics and Engineering, 15(5), 2297-2309.

Gou, B., Wang, C., Yu, T & Wang K.J. 2020. Fuzzy logic and grey clustering analysis hybrid intelligence model applied to candidate-well selection for hydraulic fracturing in hydrocarbon reservoir. Arabian Journal of Geosciences 13 (19): 975.

Guerra, E. & Yildiz, T. 2004. A Simple Approximate Method to Predict Inflow Performance of Selectively Perforated Vertical Wells. Paper SPE 89414, presented at SPE/DOE Symposium on Improved Oil Recovery. Tulsa, Oklahoma.

Hu, Y.Q., Zhao, J.Z., Ren, L. & Wang, D. 2016. Optimization of hydraulic fracture-network parameters based on production simulation in shale gas reservoirs. Journal of Engineering Research, **4** (4): 214-235.

Jamiolahmady, M., Danesh, A. & Duncan, D. B. 2006. Measurement and Modelling of Gas Condensate Flow Around Rock Perforation. Transport in Porous Media, **63** (2): 323-347.

Jamiolahmady, M., Mahdiyar, H. & Sohrabi, M. 2010. High Velocity Flow in and Around Long Perforation Tunnels. Transport in Porous Media, **84** (2): 457-469.

Jamiolahmady, M., Mahdiyar, H., Ghahria, P. & Sohrabia, M. 2011. A new method for productivity calculation of perforated wells in Gas condensate reservoirs. Journal of Petroleum Science and Engineering, **77** (3): 263-273.

Kang, Y.L, She, J.P., Zhang, H., Xu, C.Y. & You, L.J. 2016. Patterns of drilling fluid losses based on fracture propagation mechanisms of rock mass. Journal of Engineering

Research, **4** (3): 178-191.

Li, B., Sun, D. & Wu, J.H. 2012. 2D Analytical Solution of Ideal Perforation Flow. SPE Journal, **17** (2): 631-652.

Liu, X.B. 2020. A closed-form solution for stress analysis of hollow circular cylinder structure under non-uniform external load and its engineering application[J]. Journal of Engineering Research, **8** (1): 72-88.

Movahedi, H., Farahani, M.V. & Mohsen, M. 2019. Development of a Numerical Model for Single- and Two-Phase Flow Simulation in Perforated Porous Media. Journal of Energy Resources Technology, **142** (4): 042901

Muskat, M. 1943. The Effect of Casing Perforations on Well Productivity. Transactions of the AIME, **151** (1): 175-187.

Pasztor, A. & Kosztin, B. 2015. A Novel Method for Optimal Perforation Design. Paper SPE 174207, Presented at SPE European Formation Damage Conference and Exhibition, Budapest, Hungary.

Tariq, S.M. 1987. Evaluation of Flow Characteristics of Perforations Including Nonlinear Effects With the Finite-Element Method. SPE Production Engineering, **2** (2): 104-112.

Wang, Q, Hu, Y.Q., Zhao, J.Z. & Ren L. 2019. A numerical model to simulate fracture network induced by hydraulic fracturing for 3D shale gas reservoir with geo-stress interference[J]. Journal of Engineering Research, **7** (2): 45-65.

Wu, M., Zhu, J., Li, L.L. & Li, P.G. 2020. Calculation of Perforated Vertical and Horizontal Well Productivity in Low-Permeability Reservoirs. SPE Drilling & Completion, **35** (2): 218-236.

Zhang, H., Deng, Q., Li, J., Hou, X.J., Wang, H. 2018. A New Method of Estimating Penetration Depth With Different Perforation Parameters. ISRM-ARMS10-2018-063, Presented at ISRM International Symposium - 10th Asian Rock Mechanics Symposium.

Singapore.